Unsteady Flow of Non-Newtonian Fluid in a Curved Pipe With Rectangular Cross-Section

Morad M.A. and Abdul-Hadi A.M.
Department of Mathematics, College of Science, University of Baghdad. Baghdad-Iraq.

Abstract

This study is concerned with the unsteady flow of non-Newtonian, viscous, incompressible fluid in a curved pipe with rectangular cross-section, under the action of pressure gradient. An orthogonal coordinate system has been used to describe the fluid motion and it is found that the motion equations are controlled by three parameters namely; Dean number, non-Newtonian parameter and frequency parameter. Solution for the secondary flow and the axial velocity are droved as perturbation over straight pipe. Firstly the expansion was in terms of Dean number and secondly in terms of frequency parameter. Perturbation equations are solved by using variation method namely, Galerkin's method, after eliminating the dependency on time. The solutions have been developed in Cartesian coordinate for harmonic and biharmonic equations. The effect of the non-dimensional parameters mentioned above on the secondary flow, the axial velocity and the flow in the centre plane is considered. In this study we covered the steady state under consideration.

الخلاصة

في هذا البحث نتناول تحليل الجريان اللامستقر لمائع لا نيوتيني في أنبوب منحنى ذو مقطع مستطيل الشكل.لقد بينا أن ثلاثة أعداد لابعدية تتحكم بمعادلات الحركة وهي ,عدد دين,العدد اللا نيوتيني ومتغير التكرار.أستخدمت طريقة تكرارية لحل معادلات الحركة(كالريكن).قدمنا دراسة تحليلية لتأثير الاعداد الانفة الذكر على كل من الحركة الثانوية والسرعة المحورية.

Introduction

Viscous flow through straight ducts of various cross-section forms is well understood. The flow in a gently curved duct may be considered as a modification of straight axial flow in which the effect of centrifugal forces must be considered.

Dean, [5]; is that first researcher who works in flow analysis of Newtonian fluids in curved pipes. He introduced a toroidal coordinate system to show that the relation between pressure gradient and the rate of flow through a curved pipe with circular cross-section of incompressible Newtonian fluid is dependant on the curvature. In that paper he could not show this dependence but he did it in his second paper, [6]; where he modified his analysis by including higher order terms to be able to show that the rate of flow is slightly reduced by curvature.

Dean and Harst ,[7] ;obtained an approximate solution of Newtonian fluid flow in a curved pipe with rectangular cross- section assuming that the secondary motion is a uniformly stream from inner to outer bend. They modeled the equations of motion by using cylindrical coordinates. This assumption enabled them to obtain Bessel's function solution. They argued that the secondary motion decreases the rate of flow produced by a given pressure gradient and causes an outward movement at the region where the prime motion is the greatest.

In his paper Jones, [11]; makes a theoretical analysis of the flow of incompressible Non-Newtonian viscous liquid in a curved pipe with circular cross-section keeping only the first order terms. He shows that the secondary motion consists of two symmetrical vortices and the distance of the stream lines from the central plane decreases as the Non-Newtonian parameter increases.

Past work on fully developed flow in a curved square duct includes numerical studies by Mori, Uchida & Ukon, [13]; who obtained a numerical solution by using boundary-layer approximation (valid for large Dean numbers); Cheng. Lin & Ou, [4]; Ghia & Shokhey, [9]; and Joseph Smith & Adler, [12]; who obtained solutions which predicted the existence of a weak second vortex pair near the outer wall above a certain value of the Dean number. This second vortex pair was found to rotate in the opposite manner to the primary vortex pair. Cheng *et al, [*4]; predicted the onset of second vortex pair to occur when a Dean number is>150.

Ghia & Sokhey,[9] predict in it to occur above a Dean number of 143 while the calculations of Joseph *et* a/,[18] give a threshold Dean number of 152 since the curvature ratio (whose effect is embedded in the Dean number) may itself play an important role for highly curved ducts. The suitability of the Dean number as the sole parameter to characterize the onset of the second vortex pair is unclear.

For curved rectangular ducts Cheng *et al* ,[4] ; performed calculation for duct aspect ratio (defined as the ratio of height *H* to the width *B*) of 0.5, 2 and 5 for the range of the Dean number 15.9 to 312.7 at curvature ratios of 100 and 30. They reported that for an aspect ratio of 0.5 at L=176 there were no additional vortices and at L=200 there was a pair of very weak vortices close to the outer wall. In addition they found that for an aspect ratio of 5a pair of secondary vortices appeared at a rather low Dean number of 76 and the eye of the primary vortex moved toward the upper and the lower walls with the increase of Dean number.

Winters, K. H., [18]; considers the bifurcation of secondary solutions for fully developed laminar flow in curved rectangular ducts. The study is based on finite-element analysis and shows the existence of the multiple solutions arising from the non-linear equations for the range of aspect ratio from 0.8 to 1.6.

Ravi Sankar, Nandakumar & Masliyah, [14]; consider the related problems of developing flow in curved ducts. They have shown that for a range of curvature ratios and Dean numbers the flow develop into previously known two-and four- cell patterns based on fully three-dimensional calculations using the parabolized form of the Navier-Stokes equations. They have also shown that for loosely coiled ducts (of curvature ratio of 100) outside a narrow range of Dean number the solution exhibits sustained oscillations in the axial direction and that no stable steady solutions could be predicted.

Thangam and Hur, [17]; analyzed the secondary flow of incompressible viscous fluid in a curved duct by using a finite-volume method. It is shown that as Dean number is increased the secondary flow structure evolves into a double vortex pair for low -aspect- ratio duct and roll cell for duct of high aspect ratio. They found that for ducts of high curvature the onset of transition from single vortex pair to a double vortex pair or roll cells depends on the Dean number and the curvature ratio while for ducts of small curvature the onset can be characterized by Dean number alone.

Jing-Wu Wang and Andrews, [10] ; use a non-orthogonal coordinate system to study the effect of the pitch ratio and curvature on the velocity distribution of fully developed laminar flow of an incompressible fluid in a helical duct with rectangular cross-section. They used a numerical method to solve the motion equations, they find that the pitch ratio affects the pattern of the secondary flow, two-vortex become a single vortex if the pitch ratio is greater than 10 and for a certain level there will be four vortexes to appear on the plan of the cross-section.

Yakhot A., et al, [19]; studied a pulsating laminar flow of a viscous, incompressible liquid in a rectangular duct. The motion is induced under an imposed pulsating pressure difference. The problem is solved numerically. Difference flow regimes are characterized by non-dimensional parameters based on the frequency of the imposed pressure gradient oscillation and the width of the duct. The influence of the aspect ratio of the rectangular duct and the pulsating pressure gradient frequency on the phase lag, the amplitude of the induced oscillating velocity, and the wall shear were analyzed.

Abdul-Hadi, [1]; studied the unsteady flow of incompressible non-Newtonian fluid in a curved pipe with a square cross-section. He used a Galerkin method which is variational method to solve the equation of Navier-Stokes. He shown that a secondary motion depends on three dimensional parameters namely Dean number, non-Newtonian and frequency parameters, also he studied the effect of these three parameters on the secondary flow, axial velocity and some other relation.

AL-Musawy, [2]; studied the flow of non-Newtonian fluid in a curved duct with vary aspect ratio. In his

computation he used a Galerkin method and finite-difference to solve the equations of Navier-stokes. He was shown that a secondary motion depend on two dimensional parameters, also he studied the effect of non-Newtonian and aspect ratio parameters on the secondary flow and axial velocity.

Mathematical Consideration

Unsteady flow of non-Newtonian fluid in curved pipe is considered. The non-Newtonian fluid is characterized by equation of state of the form:

$$T_{ik} = 2\eta e_{ik} + 4\xi e_{ij} e_{jk} \qquad \ldots (1)$$

Where $T_{ik}, e_{ik}, \eta\ \xi$ are the stress, rate of strain, viscosity coefficient and normal stress respectively. [16]. Fig. (l) ,illustrates the coordinates system that has been used. OZ is the axis of the circle formed by the wall of the pipe. C is the center of the section of the pipe by a plane through OZ making an angle θ with a fixed axial plane. CO is the perpendicular drawn from C upon OZ and is of length R .The plane through O perpendicular to OZ and the line traced out by C will be called the central plane and the central line of the pipe respectively. Cartesian coordinates x and z are drawn in the section of the pipe, where x is parallel to OC and z parallel to OZ. The position of any point Q is then specified by cylindrical coordinate (x,θ , z), $-d \le x \le d$ and $-h \le z \le h$ where *d* and *h* are the length and height of the cross-section respectively. The Cartesian system *(X,Y,Z)* is related to the coordinate system in the cross-section by the relations

$$X = (R + x)\ Cos\ (\theta),\ Y=(R+x)Sin(\theta), Z=z \qquad \ldots(2)$$

where $o \le \theta \le 2\pi$.

Two cases will be examined for convenient length: case1 when $d = 3$, $h = 2$, see Fig. (1), and case2 when $d=2$, $h=3$ see Fig. (2)

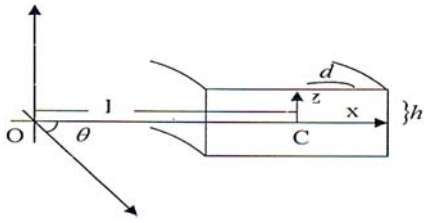

Fig. (1): Coordinates System

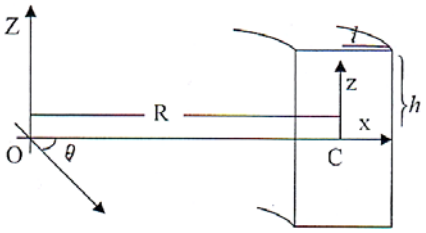

Fig. (2): coordinates System

The equation of continuity is satisfied by the introduction of a stream function ψ(x, z) such that

$$U = -\frac{\partial \psi}{\partial z}, W = \frac{\partial \psi}{\partial x} \qquad \ldots (3)$$

If we introduce non-dimensional variables for case1 by the equations

$$x_1 = \frac{x}{d}, z_1 = \frac{z}{d}, \tau = t\alpha, f = \frac{\psi}{v}, \mathrm{v} = \frac{V}{V_o} \qquad \ldots (4)$$

And for case 2

$$x_1 = \frac{x}{h}, z_1 = \frac{z}{h}, \tau = t\alpha, f = \frac{\psi}{v}, \mathrm{v} = \frac{V}{V_o} \qquad \ldots (5)$$

Where h is the characteristic length instead of d .Then from the stream function and the non-dimensional variables, it can be shown that the equations of motion may be reduce to the following partial differential equations

$$\nabla^4 f = k^2 \frac{\partial}{\partial} \nabla^2 f + L\mathrm{v}\frac{\partial v}{\partial z_1} + \left(\frac{\partial f}{\partial x_1}\frac{\partial}{\partial z_1} - \frac{\partial f}{\partial z_1}\frac{\partial}{\partial x_1}\right)\nabla^2 f - \beta L\left(\frac{\partial \mathrm{v}}{\partial x_1}\frac{\partial^2 \mathrm{v}}{\partial x_1 \partial z_1} - \frac{\partial \mathrm{v}}{\partial z_1}\frac{\partial^2 \mathrm{v}}{\partial x_1^2}\right) \qquad \ldots (6)$$

$$\nabla^4 \mathrm{v} = -2.31k^2 Cos(\tau) + k^2 \frac{\partial v}{\partial \tau} + \left(\frac{\partial f}{\partial x_1}\frac{\partial}{\partial z_1} - \frac{\partial f}{\partial z_1}\frac{\partial}{\partial x_1}\right)\nabla + \beta\left(\frac{\partial \mathrm{v}}{\partial x_1}\frac{\partial}{\partial z_1} - \frac{\partial \mathrm{v}}{\partial z_1}\frac{\partial}{\partial x_1}\right)\nabla^2 f + 2\beta\frac{\partial^2 \mathrm{v}}{\partial x_1 \partial z_1}\left(\frac{\partial^2 f}{\partial z_1^2} - \frac{\partial^2 f}{\partial x_1^2}\right) + 2\beta\frac{\partial^2 \mathrm{v}}{\partial x_1 \partial z_1}\left(\frac{\partial^2 \mathrm{v}}{\partial x_1^2} - \frac{\partial^2 \mathrm{v}}{\partial z_1^2}\right) \qquad \ldots (7)$$

And the boundary conditions are:

$$\left.\begin{array}{l} f = \dfrac{\partial f}{\partial x_1} = \dfrac{\partial f}{\partial z_1} = 0, on\ the\ boundary \\ \mathrm{v} = 0, on\ the\ boundary \end{array}\right\} \qquad \ldots (8)$$

These equations can be seen to be controlled by three parameters, a non-dimensional frequency

parameter, $k = d\left(\frac{\alpha}{\nu}\right)^2$ the non- Newtonian parameter $\beta = \frac{\xi}{\rho d^2}$ and Dean number $L = \frac{2V_0^2 d^3}{Rv^2}$. Where

$$\nabla^2 = \frac{\partial^2}{\partial x_1^2} + \frac{\partial^2}{\partial z_1^2}, \nabla^4 = \frac{\partial^4}{\partial x_1^4} + \frac{\partial^4}{\partial x_1^2 \partial z_1^2} + \frac{\partial^4}{\partial z_1^4}$$

We impose a sinusoidal pressure gradient in time with zero mean on the flow in the form of

$$-\frac{1}{R}\frac{\partial}{\partial\theta}\left(\frac{P}{\rho}\right) = JV_o \alpha Cos(\alpha t) \quad \ldots (9)$$

for convenient computation we will choose J= 2.3 1.

Where $JV_o\alpha$ the amplitude of the applied pressure gradient and α is is the angular frequency.

In what follows we shall omit the index of coordinate system, it is understood that all variables are non-dimensional form. To solve the above system, (6)-(8), we will use successive approximation method, which is equivalent to the perturbation solutions of f and v in ascending power of L . So the solution of the above system can be developed by using

$$\begin{aligned} f(x,z,t) &= Lf_1(x,z,t) + L^2 f_2(x,z,t) + .. \\ \mathrm{v}(x,z,t) &= \mathrm{v}_0(x,z,t) + L\mathrm{v}_1(x,z,t) + L^2\mathrm{v}_2(x,z,t) + .. \end{aligned} \quad \ldots (10)$$

We will limit ourselves to find the solution up to the first order in L , similar procedures can be used for higher order solutions, and the first order solution provide good accuracy for the purpose. If we substitute (10) in (6) - (8), and equate coefficients of equal power in L; we obtain a series of relations from which $\mathrm{v}_0, f_1, \mathrm{v}_1, ...$can be successively found .The equations are

$$\nabla^2 \mathrm{v}_o = k^2 \frac{\partial \mathrm{v}_o}{\partial \tau} - 2.31k^2 Cos(\tau) \quad \ldots (11)$$

$$\nabla^4 f_1 = k^2 \frac{\partial}{\partial\tau}\nabla^2 f_1 + \mathrm{v}_o \frac{\partial \mathrm{v}_o}{\partial z} - \beta\left(\frac{\partial \mathrm{v}_o}{\partial x}\frac{\partial^2 \mathrm{v}_o}{\partial x \partial z} + \frac{\partial \mathrm{v}_o}{\partial z}\frac{\partial^2 \mathrm{v}_o}{\partial z^2}\right) \ldots (12)$$

$$\nabla^2 \mathrm{v}_1 = k\frac{\partial \mathrm{v}_1}{\partial\tau} + \left(\frac{\partial f_1}{\partial x}\frac{\partial}{\partial z} - \frac{\partial f_1}{\partial z}\frac{\partial}{\partial x}\right)\mathrm{v}_o + \beta\left(\frac{\partial \mathrm{v}_o}{\partial x}\frac{\partial}{\partial z} - \frac{\partial \mathrm{v}_o}{\partial z}\frac{\partial}{\partial x}\right)\nabla^2 f_1 \ldots (13)$$

$$\nabla^2 f_1 = 2\beta\frac{\partial^2 v_o}{\partial x \partial z}\left(\frac{\partial^2 f_1}{\partial z^2} - \frac{\partial^2 f_1}{\partial x^2}\right) + 2\beta\frac{\partial^2 f_1}{\partial x \partial z}\left(\frac{\partial^2 \mathrm{v}_o}{\partial x^2} - \frac{\partial^2 v_o}{\partial z^2}\right)$$

The boundary conditions associated with the above equations, (11)-(13) are:-

$$\left.\begin{aligned} f1 = \frac{\partial f1}{\partial x} = \frac{\partial f1}{\partial z} = 0, on\ the\ boundary \\ \mathrm{v}_n = 0, n = 0.1.... \quad on\ the\ boundary \end{aligned}\right\} \quad \ldots (14)$$

By similar procedure the equations of motion for case 2 may be written as

$$\nabla^2 \mathrm{v}_o = k^2 \frac{\partial \mathrm{v}_o}{\partial \tau} - 2.31k^2 Cos(\tau) \quad \ldots (15)$$

$$\nabla^4 f_1 = k^2 \frac{\partial}{\partial\tau}\nabla^2 f_1 + \mathrm{v}_o \frac{\partial \mathrm{v}_o}{\partial z} - \beta\left(\frac{\partial \mathrm{v}_o}{\partial x}\frac{\partial^2 \mathrm{v}_o}{\partial x \partial z} + \frac{\partial \mathrm{v}_o}{\partial z}\frac{\partial^2 \mathrm{v}_o}{\partial z^2}\right) \quad \ldots (16)$$

$$\begin{aligned} \nabla^2 \mathrm{v}_1 = k\frac{\partial \mathrm{v}_1}{\partial\tau} + \left(\frac{\partial f_1}{\partial x}\frac{\partial}{\partial z} - \frac{\partial f_1}{\partial z}\frac{\partial}{\partial x}\right)\mathrm{v}_o + \beta\left(\frac{\partial \mathrm{v}_o}{\partial x}\frac{\partial}{\partial z} - \frac{\partial \mathrm{v}_o}{\partial z}\frac{\partial}{\partial x}\right)\nabla^2 f_1 \\ + 2\beta\frac{\partial^2 \mathrm{v}_o}{\partial x \partial z}\left(\frac{\partial^2 f_1}{\partial z^2} - \frac{\partial^2 f_1}{\partial x^2}\right) + 2\beta\frac{\partial^2 f_o}{\partial x \partial z}\left(\frac{\partial^2 \mathrm{v}_o}{\partial x^2} - \frac{\partial^2 v_o}{\partial z^2}\right) \end{aligned} \quad \ldots (17)$$

Where $k = h\left(\frac{\alpha}{\nu}\right)^2$, $\beta = \frac{\xi}{ph^2}$, $L = \frac{2V_0^2 h^3}{R\nu^2}$ and the boundary conditions associated with this system, (15)-(17) are

$$\left.\begin{aligned} f_1 = \frac{\partial f_1}{\partial x} = \frac{\partial f_1}{\partial z} = 0, on\ the\ boundary \\ \mathrm{v}_n = 0, n = 0,1,... \quad on\ the\ boundary \end{aligned}\right\} \quad \ldots (18)$$

Method of solution

Galerkin's method is employed to solve the equations of motion subjected to the associated boundary conditions. [3], [8], [15]

1- Solution of Case1

The motion equations (11)-(13) are solved subject to the boundary conditions (14), and as follows

1-1 Solution for $\mathrm{v_o}$

If we substitute for v_0 by the expression

$$\mathrm{v}_o = k^2\mathrm{v}_{01} + k^4\mathrm{v}_{02} + k^6\mathrm{v}_{03} + k^8\mathrm{v}_{04} + O(k^{10}) \ldots (19)$$

and equate the coefficient of equal power in k for equation (11), then the following set of equations are obtained

$$\nabla^2 \mathrm{v}_{01} = -2Cos(\tau) \quad \ldots (20)$$

$$\nabla^2 \mathrm{v}_{02} = \frac{\partial \mathrm{v}_{01}}{\partial \tau} \quad \ldots (21)$$

$$\nabla^2 \mathrm{v}_{03} = \frac{\partial \mathrm{v}_{02}}{\partial \tau} \quad \ldots (22)$$

$$\nabla^2 \mathrm{v}_{04} = \frac{\partial \mathrm{v}_{03}}{\partial \tau} \quad \ldots (23)$$

With v_{oi} =0, i =1,2,3,4 *on the boundary*.… (24)

Solution of (20) can be developed by assuming that

$$v_{01} = v_{011}(x,z)Cos(\tau) \quad \ldots (25)$$

Substituting equation (25) in (20) we get

$$\nabla^2 v_{01} = -2.31 \quad \ldots (26)$$

So the employed Galerkin's method is equivalent to the assuming of solution in the form

$$v_{011} = a_0\left(1-x^2\right)\left(\frac{4}{9}-z^2\right) \quad \ldots (27)$$

Where a_0 is a constant to be determined. It is found that the solution of (27) is

$$v_{011} = \left(1-x^2\right)\left(\frac{4}{9}-z^2\right) \quad \ldots (28)$$

Thus the complete zeroth order solution is

$$v_{01} = \left(1-x^2\right)\left(\frac{4}{9}-z^2\right)Cos(\tau) \quad \ldots (29)$$

If we substitute equation (29) in equation (21) and using the procedure of Galerkin's method, the solution of V_{o2} is found to be of the form

$$v_{02} = \left(1-x^2\right)\left(\frac{4}{9}-z^2\right)\left(a_1 + a_2x^2 + a_3z^2 + a_4x^2z^2\right)Sin(\tau) \quad \ldots (30)$$

Where a_1 a_2, a_3 and a_4 are constants.
Similarly, solution for v_{03} and v_{o4} can be found. Finally zero order solution for v_o is obtained.
The substituting of these solutions into equation (19) give; the solution for v_o ,as

$$\begin{aligned} v_0 = {} & k^2\left(1-x^2\right)\left(\frac{4}{9}-z^2\right)[Cos(\tau) + k^2(a_1 + a_2x^2 + \\ & a_3z^2 + a_4x^2z^2)Sin(\tau) + k^4(b_1 + b_2x^2 + b_3z^2 + b_4x^2z^2 \\ & b_5x^4 + b_6x^4z^2 + b_7z^4 + b_8x^2z^4 + b_9x^4z^4)Cos(\tau) + \\ & k^6(c_1 + c_2x^2 + c_3z^2 + c_4x^2z^2 + c_5x^4 + c_6x^4z^2 + \\ & c_7z^4 + c_8x^2z^4 + c_9x^4z^4 + c_{10}x^6 + c_{11}x^6z^2 + \\ & c_{12}x^6z + c_{13}z^6 + c_{14}x^2z^6 + c_{15}x^4z^6 + c_{16}x^6z^6) \\ & Sin(\tau)] + O(k^{10}) \end{aligned} \quad \ldots (31)$$

1-2 Solution for f_1:

The equation (12) contains the function v_o, which is now known through the solution (31). If we substitute v_o into (12), then that equation will contain only one unknown function which is f_1, the solution for f_1 is obtained as a perturbation in terms of the parameter *k* as follows:-

$$f_1 = k^4 f_{11} + k^6 f_{12} + O(k^8) \quad \ldots (32)$$

The recursive equations for f_1,i =1,2are obtained on equating the coefficients of equal powers in *k*. Again, we proceed to eliminate the time variable and generate a solution as an expansion in non-dimensional parameter β. Then the solution for f_1 is found to be of the form

$$f_1 = k^4(f_{111} + \beta f_{112})Cos^2(\tau) + k^6(f_{121} + \beta f_{122})Cos(\tau)Sin(\tau) + O(k^8) \quad \ldots (33)$$

1-3 Solution for v_1:

Assume that

$$v_1 = k^6 v_{11} + k^8 v_{12} + O(k^{10}) \quad \ldots (34)$$

Then the solution for v_1 is found to be of the form

$$v_1 = k^6\left[\left(v_{111} + \beta v_{112} + \beta^2 v_{113}\right)Cos^3(\tau) + k^2\left(v_{121} + \beta v_{122} + \beta^2 v_{123}\right)Cos^2(\tau)Sin(\tau)Sin(\tau) + O(k^4)\right] \quad \ldots (35)$$

Finally, substitute the solutions v_0, f_1 and v_1 into (10), the stream function and the axial velocity can be written in a convent form

$$\begin{aligned} & f(x,z,\tau) = Lf_1(x,z,\tau) \\ & f(x,z,\tau) = L[k^4(f_{111} + \beta f_{112})Cos^2(\tau) + k^6(f_{121} \\ & \qquad + \beta f_{112})Cos(\tau)Sin(\tau)] \end{aligned} \quad \ldots (36)$$

$$\begin{aligned} & v = v_0 + Lv_1 \\ & v = k^2 v_{01} + k^4 v_{02} + k^6 v_{03} + k^8 v_{04} + Lk^6(v_{111} + \\ & \beta v_{112} + \beta^2 v_{113})Cos^3(\tau) + Lk^8(v_{121} + \beta v_{122} + \\ & \beta^2 v_{123})\}Cos(\tau)^2 Sin(\tau) \end{aligned} \quad \ldots (37)$$

where all the above f 's and v's are polynomials in x and z.
If f and v are independent of t and $k = 1$ the system (11)-(13) will be reduced to corresponding system in case of steady state.

2- Solution of case2

By similar procedure the solution of case 2 for the stream function and the axial velocity are

$$\begin{aligned} & f(x,z,\tau) = Lf_1(x,z,\tau) \\ & f(x,z,\tau) = L[k^4(f_{111} + \beta f_{112})Cos^2(\tau) + k^6(f_{121} \\ & \qquad + \beta f_{112})Cos(\tau)Sin(\tau)] \end{aligned} \quad \ldots (38)$$

$$\begin{aligned} & v = v_0 + Lv_1 \\ & v = k^2 v_{01} + k^4 v_{02} + k^6 v_{03} + k^8 v_{04} + Lk^6(v_{111} + \\ & \beta v_{112} + \beta^2 v_{113})Cos^3(\tau) + Lk^8(v_{121} + \beta v_{122} + \\ & \beta^2 v_{123})Cos(\tau)^2 Sin(\tau) \end{aligned} \quad \ldots (39)$$

Where all the above f's and v's are polynomials in x and z.
Also if f and v are independent of t and $k = 1$ the system (15)-(17) will be reduced to corresponding system in case of steady state.

Results and Discussion

The secondary flow occurs in curved ducts or curved pipes. Physically the parameter L (Dean number) can be considered as the ratio of the centrifugal force induced by circular motion of the fluid to viscous force when a fluid flows through a curved pipe. Pressure gradient directed towards the center of curvature, is setup across the pipe to balance the centrifugal force arising from curvature. The fluid near the wall of the pipe is moving more slowly than the fluid some way from the wall owing to viscosity and therefore require small pressure gradient to balance the local centrifugal force. As a result of these different pressure gradients, the faster-flowing fluid moves outwards, whilst the slower-flowing fluid moves inward. This flow is known as the secondary flow and it is superposed on the main stream region towards the outer wall and creating a much thicker layer of slowly moving fluid at the inner wall, however, owing the enhanced mixing and momentum transfer due to the secondary flow, the total frictional loss of energy near the wall increases and the fluid experiences more resistance in posing through the pipe.

1- Streamline Projection for Case1

The differential equations of the streamline is,

$$\frac{dX}{U} = \frac{(R+x)d\theta}{V} = \frac{dZ}{W} \qquad \dots (40)$$

The velocity components, *(U, V, W)* are to be obtained from equations (36) and (37). Up to sufficient accuracy equation (40) may be written as

$$\frac{dX}{U} = \frac{Rd^4 d\theta}{V_o\left(1-x^2\right)\left(\frac{h^2}{d^2}-z^2\right)} = \frac{dZ}{W} \qquad \dots (41)$$

It is clear that all the variables are in the dimensional form.

1-1 Streamline Projection in the Central Plane:

The motion of the liquid in the central plane of the pipe is of special simplicity .At any point on OC we have z = 0 and $\partial\psi/\partial x = 0$, $-1 \le x \le 1$ which mean that w vanishes; (i.e. the liquid particles located in the central plane do not possess the w component of velocity which is responsible of moving them out of this (x = 0) plane). As a result the direction of the velocity at such point in the liquid lies in the central plane. Thus the motion in the upper half of the pipe is quite distinct from that in the lower half and it is clear that the central plane is the plane of symmetry for the motion.
The differential equation of the streamline in the central plane is

$$\frac{dx}{U} = \frac{Rd^2 d\theta}{V_o \frac{h^2}{d^2}\left(d^2-x^2\right)} \qquad \dots (42)$$

From the dimensional analysis we have

$$U = \frac{vu}{d} \qquad \dots (43)$$

Then by suing equations (43) and (10) we obtain

$$U = \frac{vL}{d}\frac{\partial f_1}{\partial z} \qquad at\ z = 0 \qquad \dots (44)$$

Where $L = 2R_e^2\left(\frac{d}{R}\right)$

Substituting equation (44) into equation (42) we obtain

$$\frac{dx_1}{d\theta} = \frac{-2R_e}{\frac{h^2}{d^2}\left(1-x_1^2\right)} \cdot \left.\frac{\partial f_1}{\partial z}\right|_{z=0} \qquad \dots (45)$$

Where $Re = V_o\, d/\nu$, is Reynolds number which specify the nature of flow.
Substituting for f_1 from (36) into (45) and solving the resulting differential equation we obtain

$$\theta = \frac{1}{\frac{16}{9}R_e(a_2+\beta b_1)h\left(h^2-1\right)} \cdot \ln\left[\left(\frac{1+x}{1-x}\right)^h \cdot \left(\frac{h+x}{h-x}\right)\right]$$

... (46)

Where

$$h = \left(\frac{a_1+\beta b_3}{a_2+\beta b_1}\right) < 0\,,\ \beta \in (-\infty,\infty)/[-0.16,0.044]$$

And

$$\theta = \frac{-h^2}{\frac{16}{9}R_e(a_2+\beta b_1)h\left(h^2+1\right)}\left[\ln\left(\frac{1+x}{1-x}\right)^h + \tan^{-1}\left(\frac{x}{h}\right)\right]$$

... (47)

Where

$$h = \left(\frac{a_1 + \beta b_3}{a_2 + \beta b_1} \right) < 0 \, , -0.16 \le \beta < 0.044$$

Here θ is measured from the point where the streamline cross the central plane (x = 0) . The (x, θ) relation is independent of the dimension of the cross-section.

For a given value of x, the range of θ varies with the dimensionless parameters Re and β, in the case of Newtonian fluid (β= 0)the range of θ varies inversely with Re and for a fixed value of Re the range of θ increase as β decreases. It is found that an increase in β leads to a decrease in the curvature of the streamlines in the central plane.

It is noted that the value of θ increases steadily with x and tends to infinity as x tends to unity and θ tends to minus infinity as x tends to minus one.

Numerical illustration is now given for a particular boundary and Reynolds number considered by Dean [5], namely Re =63.3, $\frac{d}{R} = \frac{1}{3}$ and for different values of the parameters β,k,L and time τ.

Fig. (3, 4), illustrate the streamline projection in the central plane. The streamline grows smoothly along the central plane and merges with the outer wall of the pipe. This shape is greatly affected by the nonlinear stresses. The non-linear stresses force the flow to be around the inner wall for a quite angular distance, the flow centrifugal force forces the direction to sharply move in a radial direction but the flow steers near the outer wall again. This phenomenon becomes very clear asβ, the non-Newtonian parameter, increase through the interval (-∞,∞)\ [-0.16, 0.044], see Fig. (3). inversely it is disappearing as β varies from -0.16 to 0.044 Fig. (4)

1-2 Streamline Projection on the Cross-Section of the Pipe:

The streamline projection on the cross-section for a curved pipe are represented by

f_1 = Constant

Where f_1 is given by (36), which is combination of the radial and vertical velocity. The nature of the closed curved streamline for various fluid changes because of the non-Newtonian parameter.

The factors that affected on the secondary flow and θ -component velocity as can be seen from equations (36) and (37) are the frequency parameter k, the non-Newtonian parameterβ, Dean number D and the time τ.

Sixty eight cases have been studied to cover the effect of each of these factors on the secondary flow and θ -component velocity. All figures (7-30) show that, there are two symmetrical regimes of secondary flow to appear in the cross-section in curved pipe. Also, it is noted that the intensity of the secondary flow is stronger in the middle of each of the upper and lower of the cross-section and becomes weaker when the more toward the boundary and the central plane.

For β increase through the interval (-∞,∞)\ [-0.16, 0.044], k = l.77 and L = 0.01 it is found that there is small vertical displacement away from the central plane, and the intensity of the secondary flow increases, see Fig. (7, 8).

In fig. (9-12) when β = 1 and for k and L greater than zero, it is noted that the effect of k and L on the displacement of the secondary flow is the same as the effect of β and the intensity of secondary flow increase as k and L increase, but when ft is small, e.g. β = 0.044 and different values of k and L, there is no displacement but there is change in intensity of the stream function, see Fig. (13-16).

Fig. (17-30) illustrated the effect of time on the streamline projection on the cross-section in curved pipe. In fig. (17-24), the values of β,k and L are 1, 1.77, and 0.01 respectively and τ varies from 0 to 6.28. As τ varies from 0 to 2.05 (τ is measured in radian) there is displacement toward the central plane and the streamline become thicker near the central plane, see Fig. (17-19).

The transition stage from a two-vortex structure to a four-vertex structure occurs at τ = 2.061; where two additional vortices start to grow near the corner of the inner and outer walls, see Fig (20). They are clearer at τ = 2.07, see Fig. (21) and the twin vortices rotating in opposite direction of the main vortices appear. Also, at τ increase it is noted that there are two stagnation regions near the corner of the inner and outer walls, Fig. (20), moving toward the center of the cross-section, Fig. (21). As τ increases, it is observed that the vortices in upper and lower half of cross-section near the corner of the inner and outer walls of the pipe expand and make another secondary flow, because of continuity displacement of the main vortices toward the central plane as τ increase, the new vortices control to the flow in pipe and become the main vortices, Fig.(22-24).

When the value of β is small, e. g. 0.044, and for the same values of k and L (i.e. k = l.77 and L = 0.01), the increasing in τ from 0 to 6.28 lead to growth one vertex in each halve of the cross-section (upper and lower the central plane) near

the boundaries, the vertices appear at $\tau \cong 1.75$, Fig.(26), and its direction opposite to main vortices. At τ varies from 0 to 6.28, the main vertices displace to the central plane. So it reaches to stagnation regions, inversely the vertices that appear in upper and lower cross-section growth to take the location of the main vertices, see Fig. (25-30).

1-3 The Effect of Parameters, (β, k, L) and time τ) on θ- Component Velocity:

The effect of parameters, (β,k,L and τ) on θ-component velocity illustrated in Fig.(35-47). It is noted that, parametersβ, k and τ have weak effect on the location of center of axial velocity, and the increase in β and k leads to an increase on the value of the axial velocity. For increasing L there is horizontal displacement in the center of the axial velocity toward the outer wall of the pipe, see Fig.(31-38). In Fig.(40-43) we noted that for small value for β, (β = 0.044), and the increase in k leads to increase in the intensity of the axial velocity but the increase in β and L have not effected, see Fig.(41,42).

2- Streamline Projection for Case2

As in case1, the differential equations of the streamline are

$$\frac{dX}{U} = \frac{(R+x)d\theta}{V} = \frac{dZ}{W} \qquad \dots (48)$$

The velocity components, (U, V, W) are to be obtained from equations (38) and (39). Up to sufficient accuracy equation (48) may be written as

$$\frac{dX}{U} = \frac{Rd^4 d\theta}{V_o\left(\frac{d^2}{h^2} - x^2\right)\left(1 - z^2\right)} = \frac{dZ}{W} \qquad \dots (49)$$

Also the expressions here appear in dimensional form.

2-1 Streamline Projection in the Central Plane:

This section has the same properties in the previous section for case1 and the differential equation of the streamline in the central plane is

$$\frac{dx}{U} = \frac{Rd^2 d\theta}{V_o\left(d^2 - x^2\right)} \qquad \dots (50)$$

In case 2 equation (43) becomes

$$U = \frac{vu}{h} \qquad \dots (51)$$

Using equations (51) and (10) we obtain

$$U = \frac{vL}{h}\frac{\partial f_1}{\partial z} \qquad at\ z = 0 \qquad \dots (52)$$

Where $L = 2\,\mathrm{Re}^2\left(\frac{h}{R}\right)$

Substituting equation (52) into equation (50), gives

$$\frac{dx_1}{d\theta} = \frac{-2\,\mathrm{Re}}{\left(\frac{h^2}{d^2} - x_1^2\right)} \cdot \left.\frac{\partial f_1}{\partial z}\right|_{z=0} \qquad \dots (53)$$

Substituting for f_1 from (38) into (53) and solving the resulting differential equation gives

$$\theta = \frac{1}{4.\,\mathrm{Re}(a_2 + \beta b_1)h\left(h^2 + \frac{4}{9}\right)} . ln\left[\frac{3}{2}\ln\left(\frac{2/3 + x}{2/3 - x}\right)^h + 2\tan^{-1}\left(\frac{h - x}{h + x}\right)\right]$$

$$\dots (54)$$

Where

$$h = \left(\frac{a_1 + \beta b_3}{a_2 + \beta b_1}\right) < 0\,,\ \beta \in (-\infty, \infty)/[-0.16, 0.025]$$

And

$$\theta = \frac{-h^2}{4\,\mathrm{Re}(a_2 + \beta b_1)h\left(h^2 + \frac{4}{9}\right)} . ln\left[\frac{3}{2}\ln\left(\frac{2/3 + x}{2/3 - x}\right)^h + 2\tan^{-1}\left(\frac{x}{h}\right)\right]$$

$$\dots (55)$$

Where

$$h = \left(\frac{a_1 + \beta b_3}{a_2 + \beta b_1}\right) < 0\,,\ \text{and}\ -0.16 \le \beta < 0.025$$

It noted that 0 has the same properties as in section (4.2.1), but it tends to infinity as x tends to $2/3$ and it is tend to minus infinity as x tends to -$2/3$.

From fig. (5, 6), we noted that the stream line projection in the center plane has the same phenomenon describe in section (4.2.1) associated with similar effect of β but in slowly form.

2-2 Streamline Projection on the Cross-Section of the Pipe:

Figures (44-60) illustrate the effect of β, k, L and τ on the stream line projection' on the cross-section in a curved pipe. It is found that there is no

displacement in a secondary flow as β , k and L increase.

In addition, it is found that the intensity of the secondary flow increases as β, k and L increase, see Fig.(44-49). Also, it is noted that there are two stagnation regions near the inner and outer walls moving toward the center of cross-section as β , k and L increase.

As τ increases and the values of β, k and L are 10, 1.77 and 0.01 respectively, there is displacement toward the boundaries and the streamlines become thicker near the boundaries, Fig. (50). The transition stage from a stage from a two-vortex structure to a four-vertex structure occurs at τ= 1 .85 ; where two additional vortices start to grow near the inner and outer walls, see Fig.(51), the twin vortices rotating in opposite direction of the main vortices appear. Also, at τ increase it is noted that there are two stagnation regions near the inner and outer walls moving toward the center of the cross-section, see Fig.(50).

For τ >1.85, the stagnation regions start to move toward the center of cross-section causes displacement to main vortices toward the boundaries with the new vortices near the inner and outer walls move toward the center of cross-section to reach the main vortices, see Fig.(52-54).

Fig.(55-60), illustrate the effect of k, L and τ when β is small such as β=0.024, it is noted that there is small displacement toward the central plane as β, k , L and τ increases and the intensity increase as these factors increase.

Finally, it is observed that the effect of each of the factors (β, k , L and τ) on θ-component velocity have the same effect in case1 (except L has stronger effected than in case1) see Fig.(61-74).

Comparison between Case1 and Case2 with Some Conclusions

For streamline projection in a central plane of the pipe, it is noted that as β increases, the effect in case1 is stronger than case2.

Regarding streamline projection in the cross-section, in case l it is noted that the increase in β, k and L lead to a weak displacement away from center plane and the intensity increases as these factors increase, while in case2, the increase in these factors lead to increase in the intensity (different from that in case l) of the secondary flow but there is no displacement.

In addition to that, in case1 the increase in τ leads to a displacement toward the central plane and the streamline become thicker near central plane.

At τ = 2.061 -there exist four-vortex structure near the corner of the inner and outer walls of the pipe; while in case2, the displacement was toward the boundaries occur and the streamline become thicker near the boundaries as τ increase. The four-vortex structure near the inner and outer wall appear at τ =1.85. Also, for small values of β, in case1 it is noted that there exist two-vortex structure and the displacement toward the central plane but there is no such they in case2.

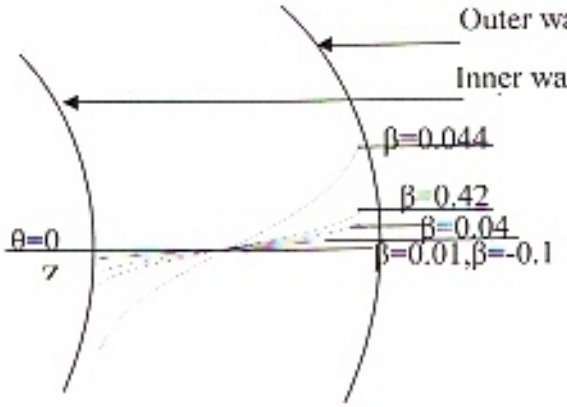

Fig.(3),streamline projection in the central plane for β =-.1, 0.01, 0.04, 0.042, 0.044

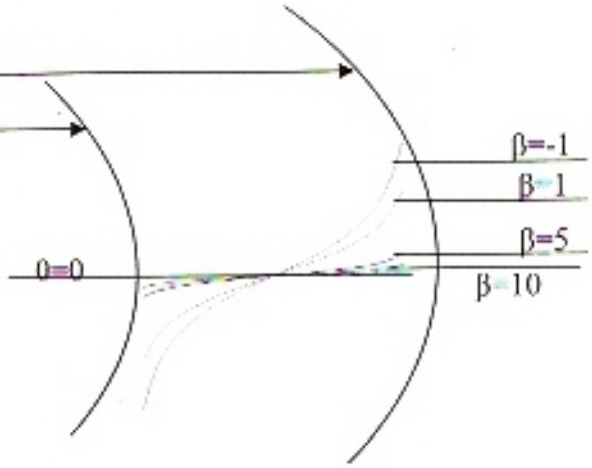

Fig.(4),streamline projection in the central plane for β =-1, 1, 5, 10

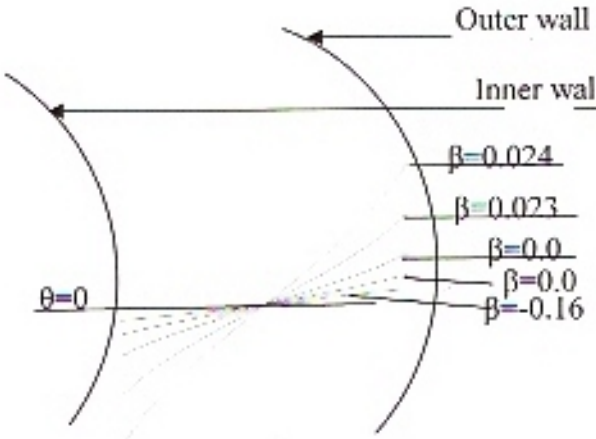

Fig.(5),streamline projection in the central β =-.16, 0.01, 0.02, 0.023, 0.024

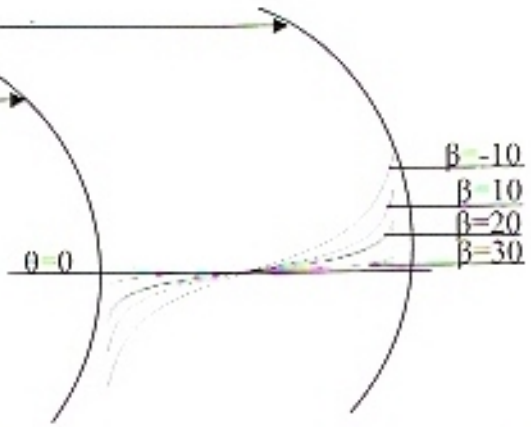

Fig.(6),streamline projection in the plane for central plane for β =-10, 10, 20, 30

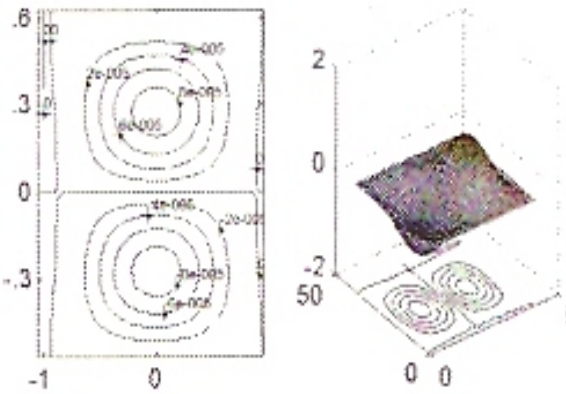

Fig.(7),paths of particales projected on the cross-section for β=-1,k=1.77,L=0.01, τ=0.39

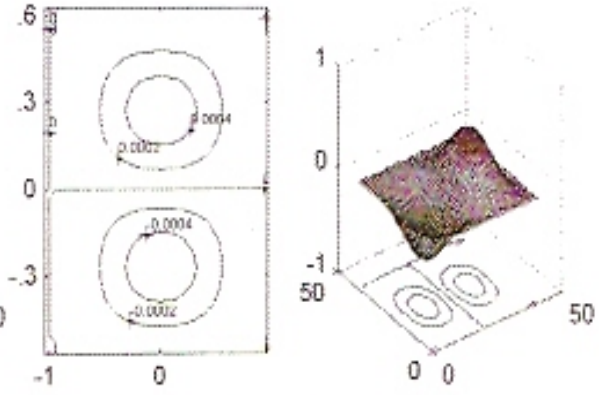

Fig.(8),paths of particales projected on the cross-section for β=5,k=1.77,L=0.01, τ=0.39

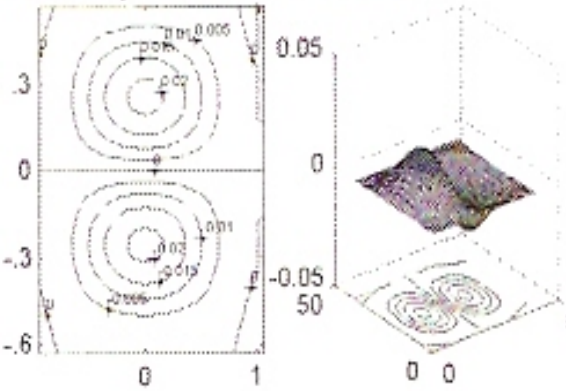

Fig.(9),paths of particales projected on the cross-section for β=1,k=5.1,L=0.01 τ=0.39

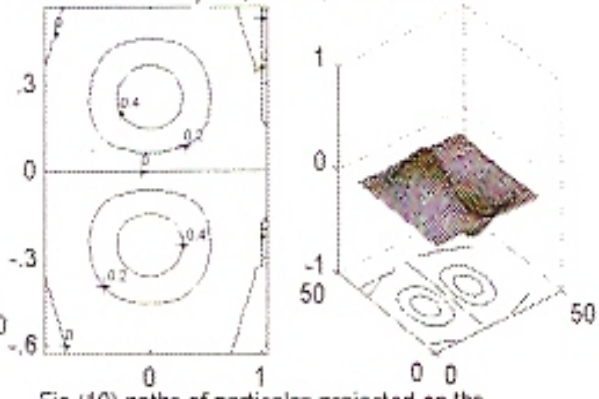

Fig.(10),paths of particales projected on the cross-section for β=1,k=9,L=0.01,τ=0.39

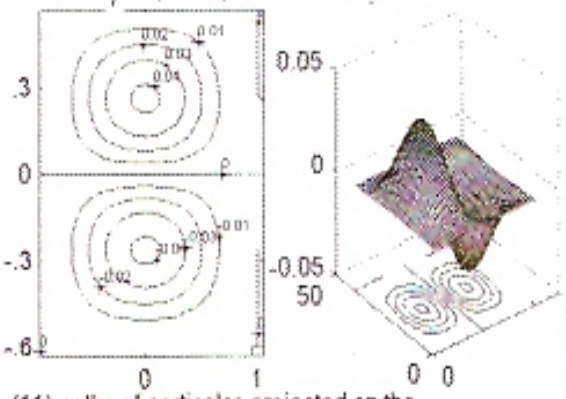

Fig.(11),paths of particales projected on the cross-section for β=1,k=1.77,L=3.36, τ=0.39

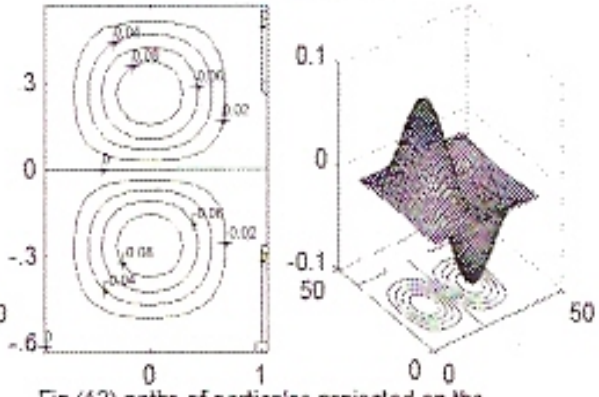

Fig.(12),paths of particales projected on the cross-section for β=1,k=1.77,L=8, τ=0.39

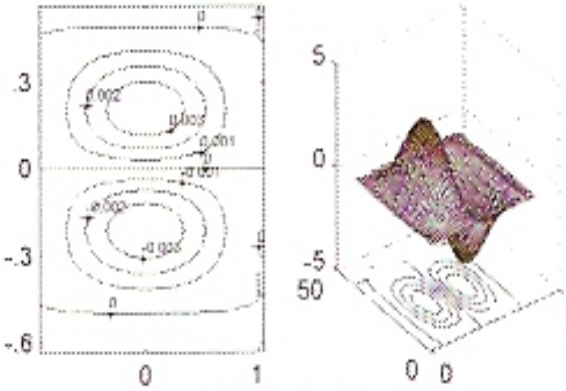

Fig.(13),paths of particales projected on the cross section for β=0.044,k=5.1,L=0.01, τ=0.39

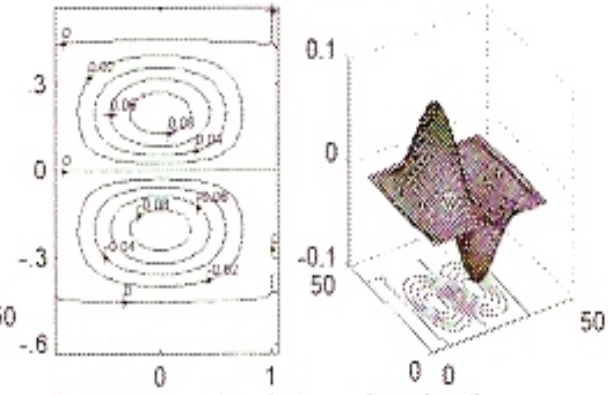

Fig.(14),paths of particales projected on the cross-section for β=0.04,k=9,L=0.01, τ=0.39

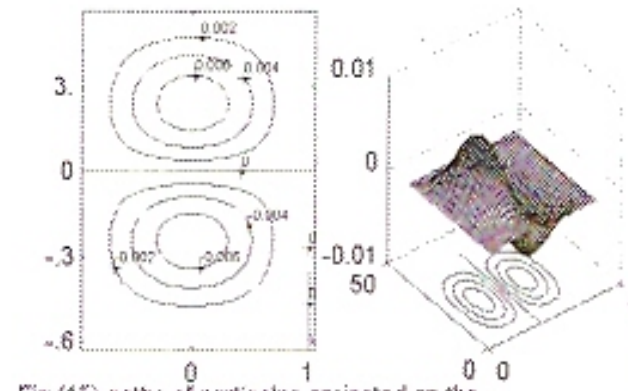

Fig.(15),paths of particales projected on the cross-section for β=0.044,k=1.77,L=3.36,τ=0.39

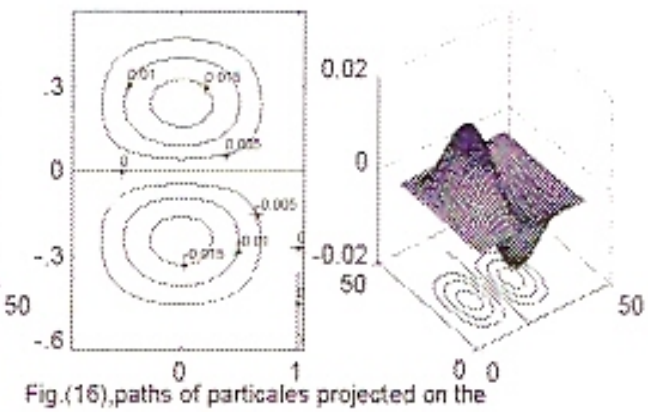

Fig.(16),paths of particales projected on the cross-section for β=0.044,k=1.77,L=8,τ=0.39

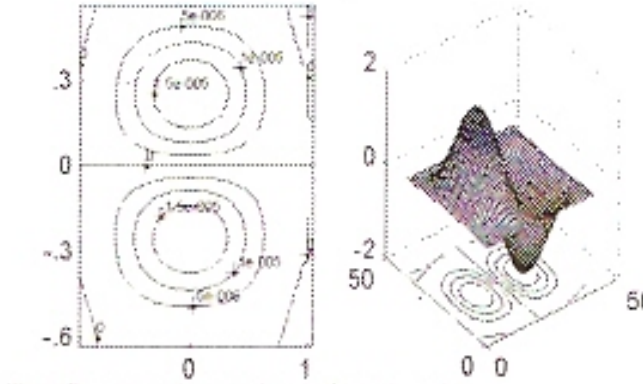

Fig.(17),paths of particales projected on the cross-section for β=1,k=1.77,L=0.01,τ=1.36

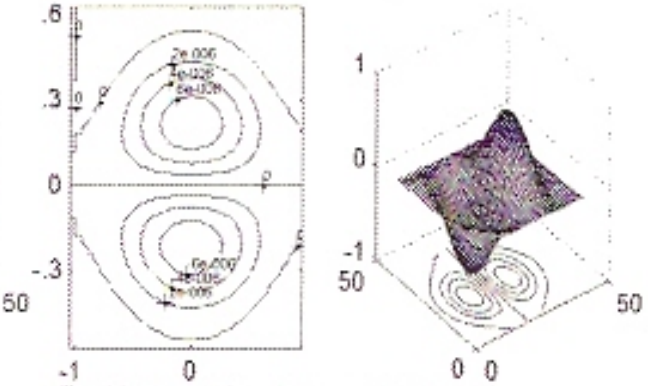

Fig.(18),paths of particales projected on the cross-section for β=1,k=1.77,L=0.01,τ=2

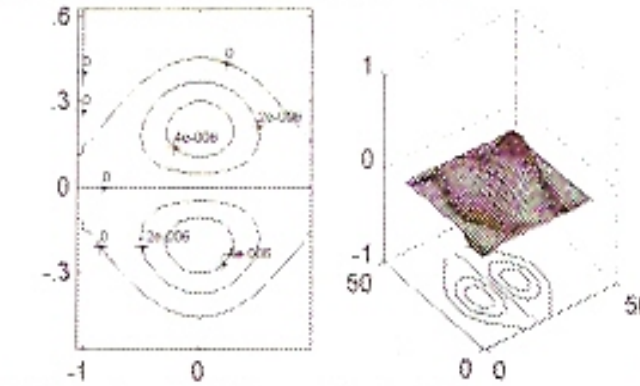

Fig.(19),paths of particales projected on the cross-section for β=1,k=1.77,L=0.01,τ=2.05

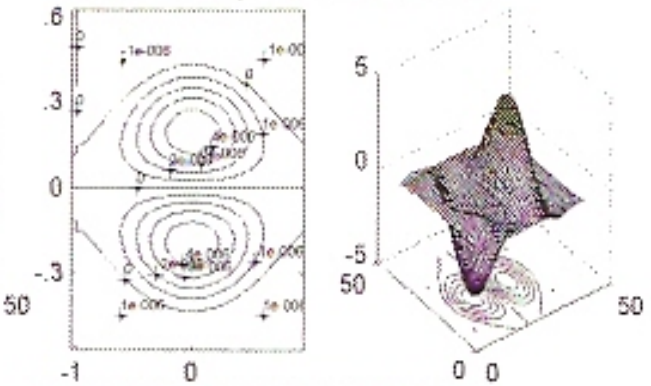

Fig.(20),paths of particales projected on the cross-section for β=1,k=1.77,L=0.01,τ=2.061

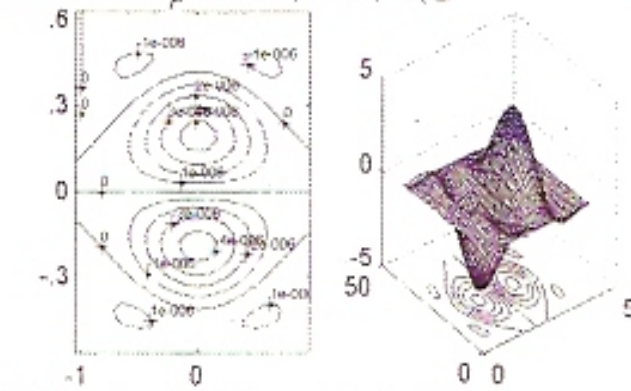

Fig.(21),paths of particales projected on the cross-section for β=1,k=1.77,L=0.01,τ=2.07

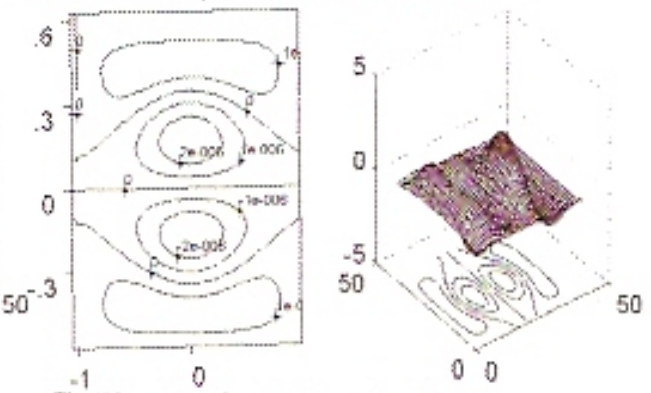

Fig.(22),paths of particales projected on the cross-section for β=1,k=1.77,L=0.01,τ=2.1

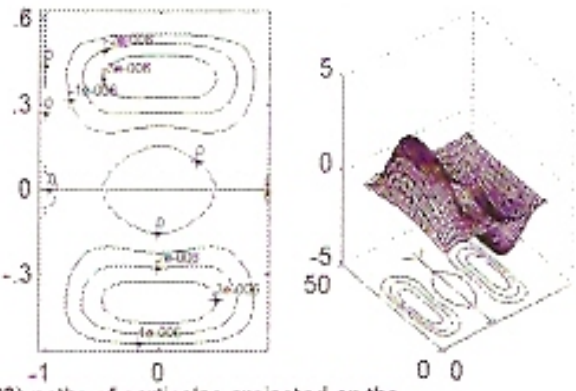

Fig.(23),paths of particales projected on the cross-section for β=1,k=1.77,L=0.01, τ=2.15

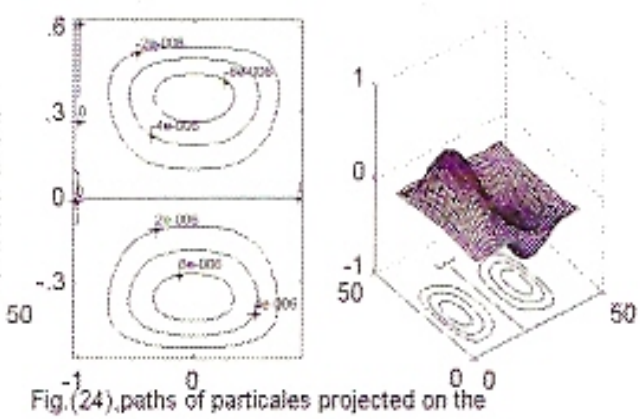

Fig.(24),paths of particales projected on the cross-section for β=1,k=1.77,L=0.01,τ=2.2

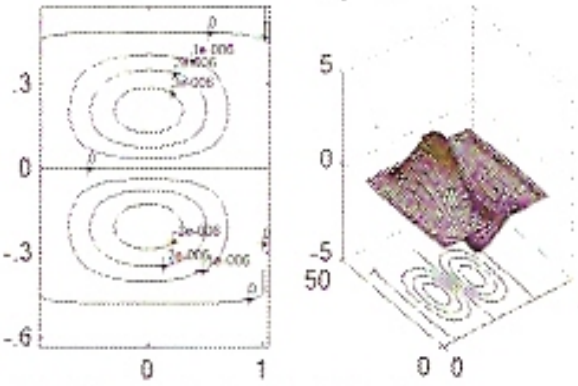

Fig.(25),paths of particales projected on the cross-section for β=0.044,k=1.77,L=0.01, τ=1.36

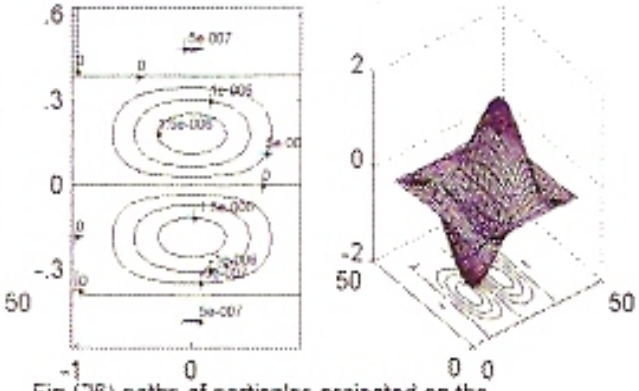

Fig.(26),paths of particales projected on the cross-section for β=0.044,k=1.77,L=0.01, τ=1.753

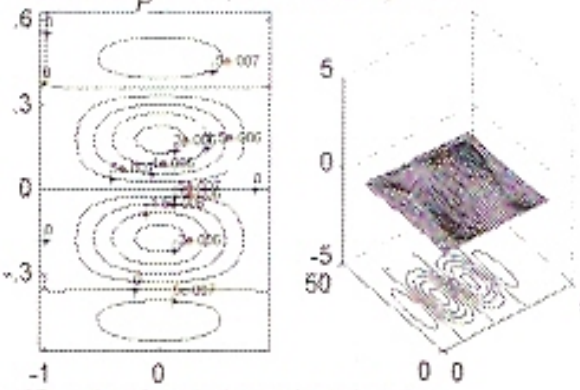

Fig.(27),paths of particales projected on the cross-section for β=0.044,k=1.77,L=0.01 τ=1.85

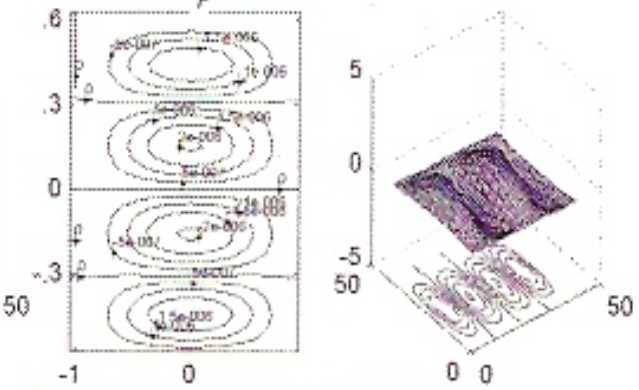

Fig.(28),paths of particales projected on the cross-section for β=0.044,k=1.77,L=0.01, τ=2

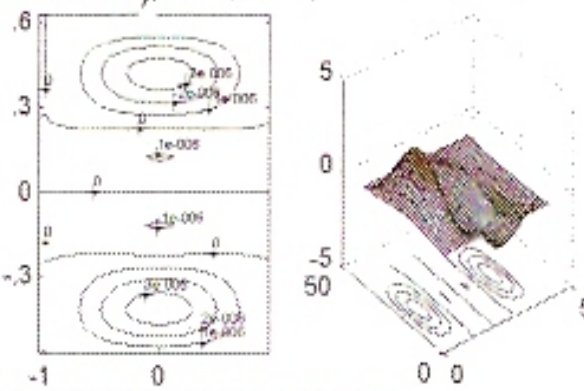

Fig.(29),paths of particales projected on the cross-section for β=0.044 k=1.77,L=0.01, τ=2.1

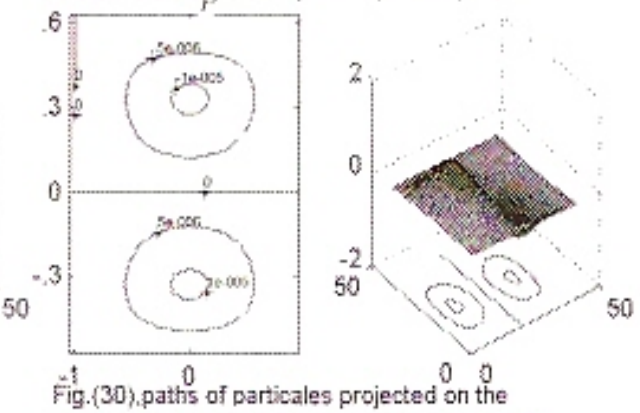

Fig.(30),paths of particales projected on the cross-section for β=0.044,k=1.77,L=0.01, τ=2.6

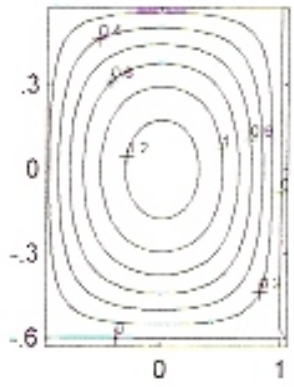

Fig.(31),axial velosity for β=5,k=1.77,L=0.01, τ=0.39

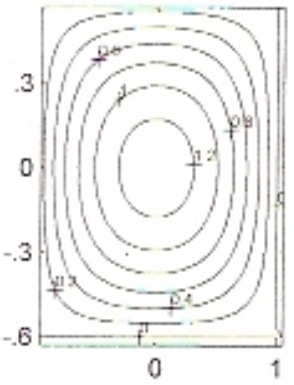

Fig.(32),axial velosity for β=-1,k=1.77,L=0.01,τ=0.39

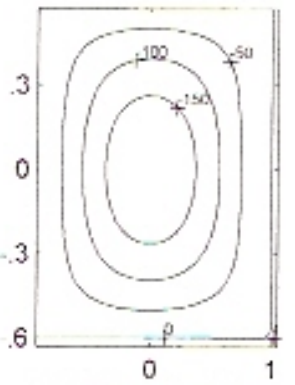

Fig.(33),axial velosity for β=1,k=5.1,L=0.01,τ=0.39

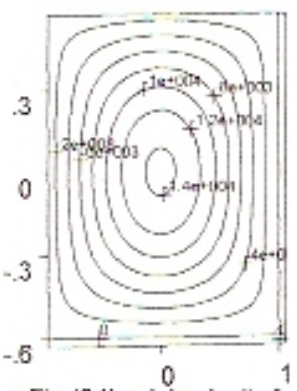

Fig.(34),axial velosity for β=1,k=9,L=0.01,τ=0.39

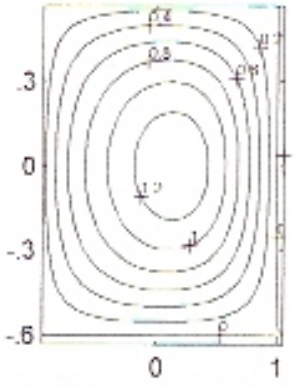

Fig.(35),axial velosity for β=1,k=1.77,L=3.36,τ=0.39

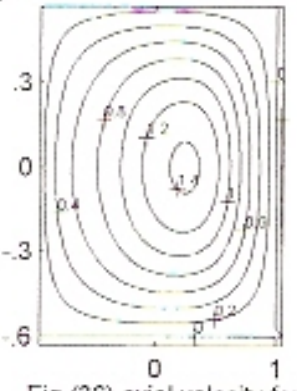

Fig.(36),axial velosity for β=1,k=1.77,L=8,τ=0.39

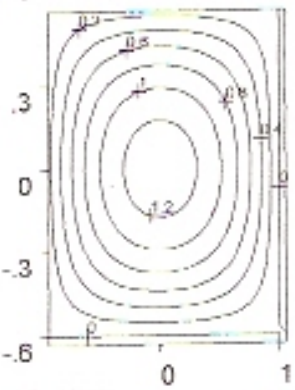

Fig.(37),axial velosity for β=1,k=1.77,L=0.01,τ=0.39

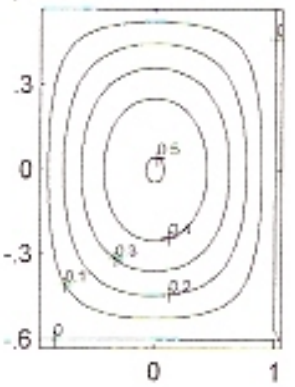

Fig.(38),axial velosity for β=1,k=1.77,L=0.01,τ=1.57

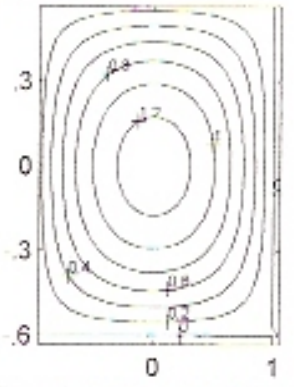

Fig.(39),axial velosity for β=0,k=1.77,L=0.01, τ=0.39

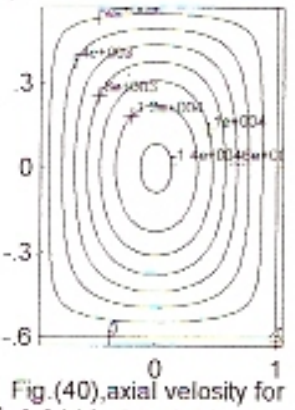

Fig.(40),axial velosity for β=0.044,k=9,L=0.01,τ=0.39

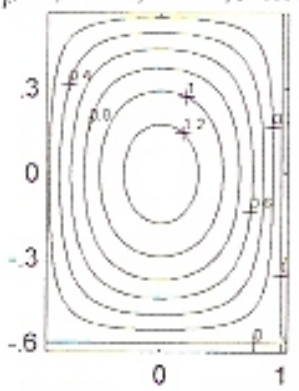

Fig.(41),axial velosity for β=0.044,k=1.77,L=3.36, τ=0.39

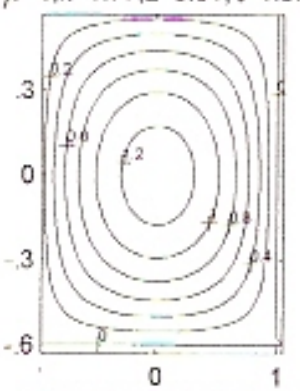

Fig.(42),axial velosity for β=8,k=1.77,L=0.01, τ=0.39

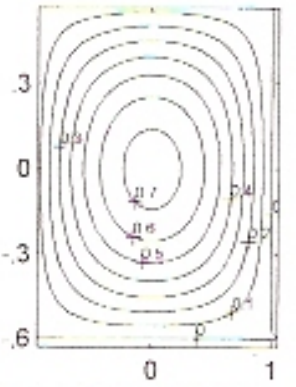

Fig.(43),axial velosity for β=0.044,k=1.77,L=0.01,τ=1.36

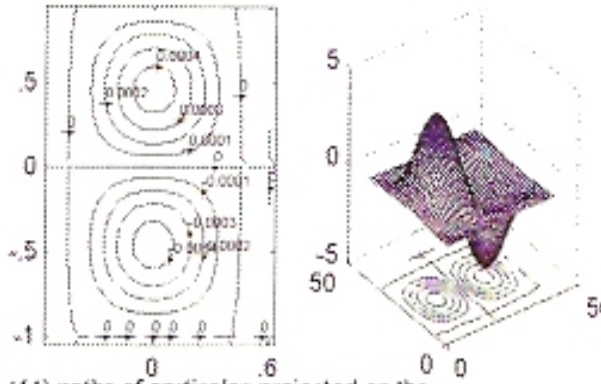

Fig.(44),paths of particales projected on the cross-section for β=10,k=1.77,L=0.01, τ=0.39

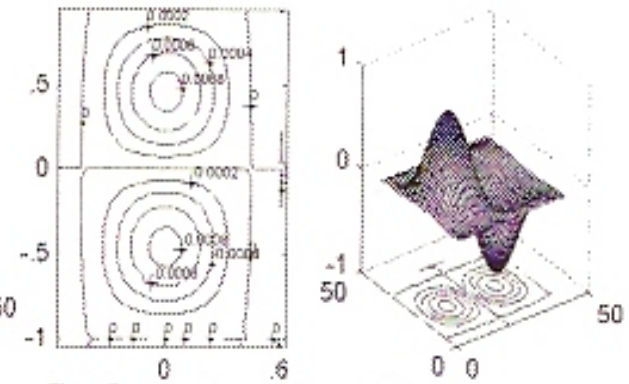

Fig.(45),paths of particales projected on the cross-section for β=20,k=1.77,L=0.01, τ=0.39

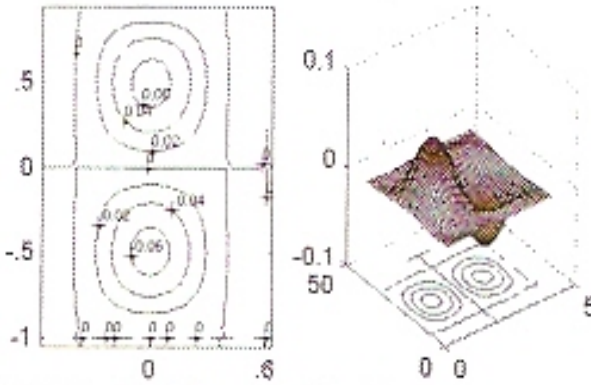

Fig.(46),paths of particales projected on the cross-section for β=10,k=5.1,L=0.01, τ=0.39

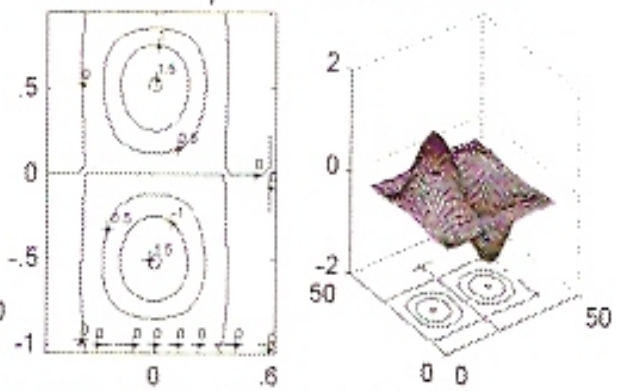

Fig.(47),paths of particales projected on the cross-section for β=10,k=9,L=0.01, τ=0.39

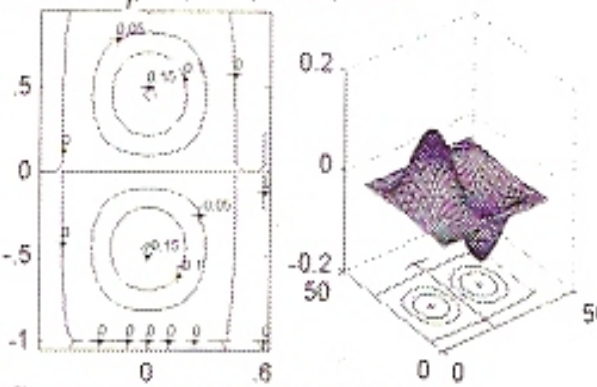

Fig.(48),paths of particales projected on the cross-section for β=10,k=1.77,L=3.36, τ=0.39

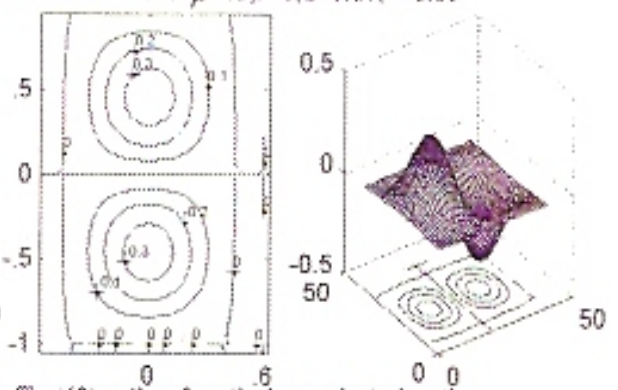

Fig.(49),paths of particales projected on the cross-section for β=10,k=1.77,L=8 τ=0.39

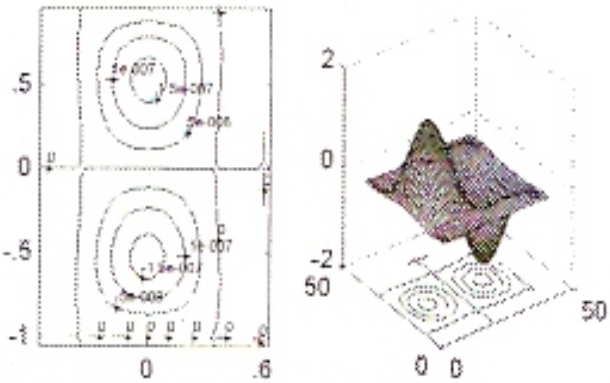

Fig.(50),paths of particales projected on the cross-section for β=10,k=1.77,L=0.01, τ=1.57

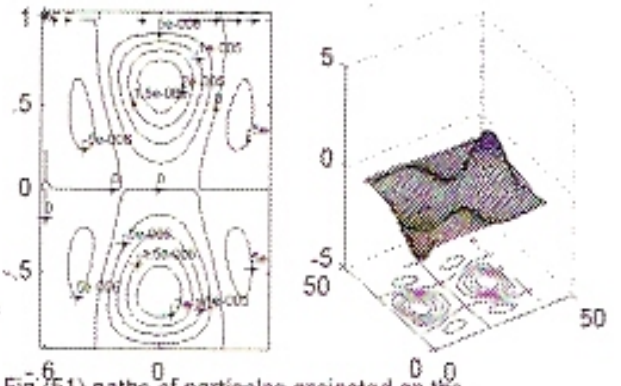

Fig.(51),paths of particales projected on the cross-section for β=10,k=1.77,L=0.01, τ=1.85

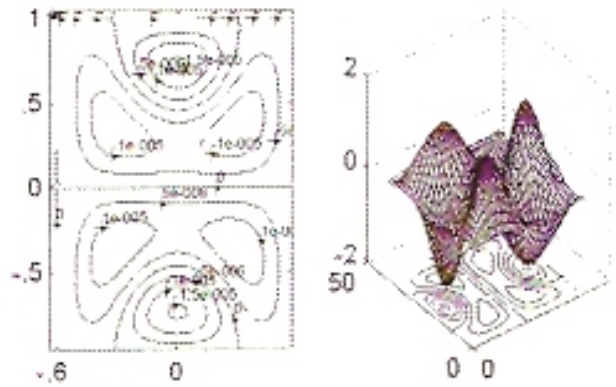

Fig.(52),paths of particales projected on the cross-section for β=10,k=1.77,L=0.01, τ=2

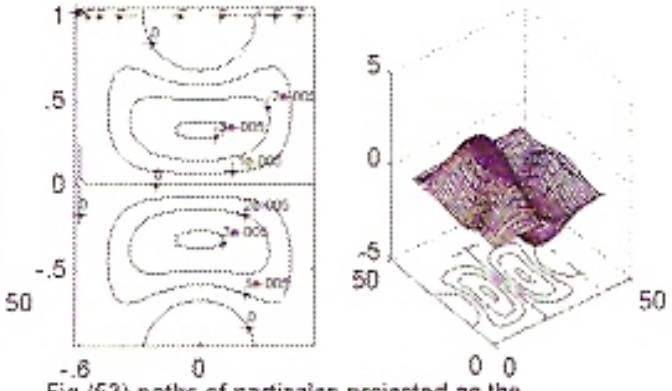

Fig.(53),paths of particales projected on the cross-section for β=10,k=1.77,L=0.01,τ=2.1

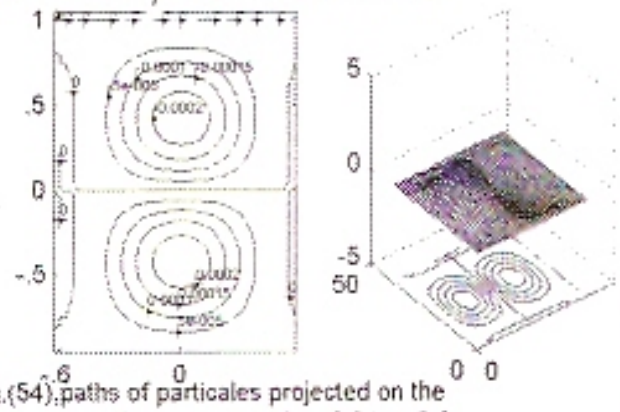

Fig.(54),paths of particales projected on the cross-section for β=10,k=1.77,L=0.01, τ=2.6

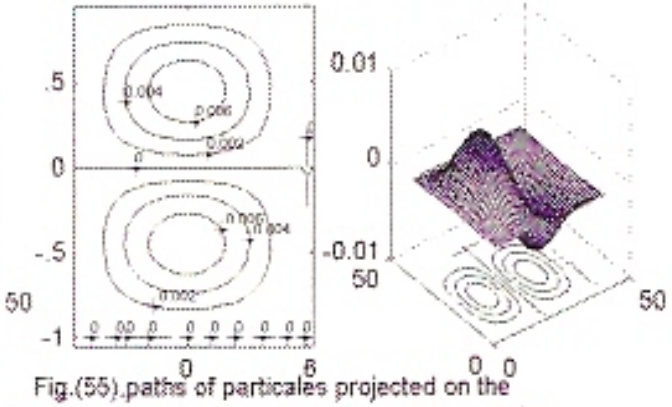

Fig.(55),paths of particales projected on the cross-section for β=0.024,k=5.1,L=0.01, τ=0.39

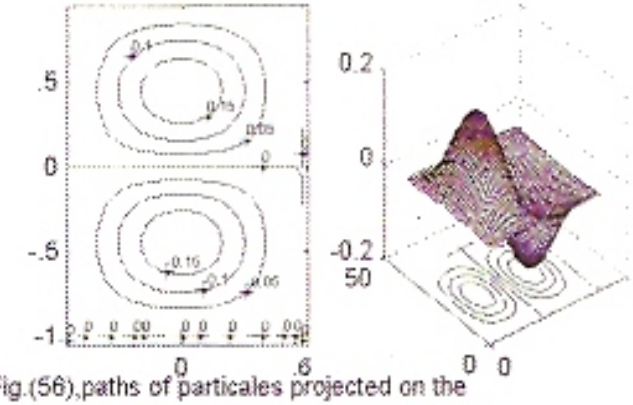

Fig.(56),paths of particales projected on the cross-section for β=0.024,k=9,L=0.01, τ=0.39

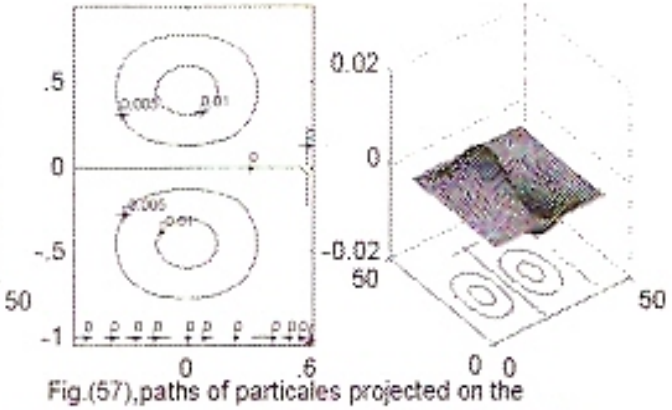

Fig.(57),paths of particales projected on the cross-section for β=0.024,k=1.77,L=3 36, τ=0.39

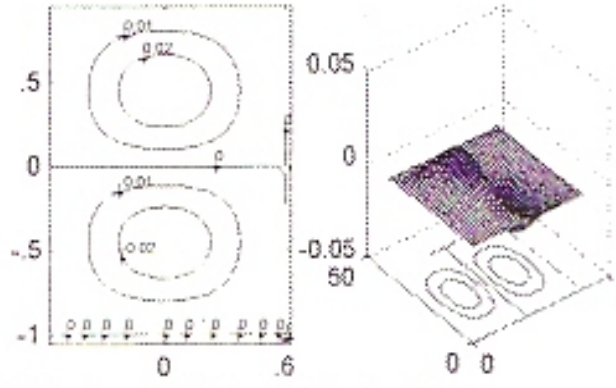

Fig.(58),paths of particales projected on the cross-section for β=0.024,k=1.77,L=8,τ=0.39

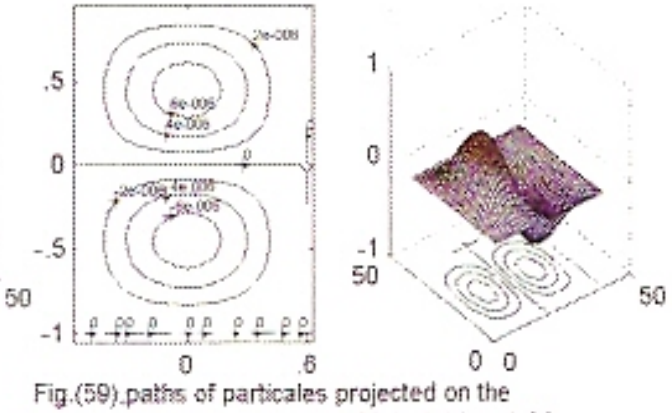

Fig.(59),paths of particales projected on the cross-section for β=0.024,k=1.77,L=0.01,τ=1.36

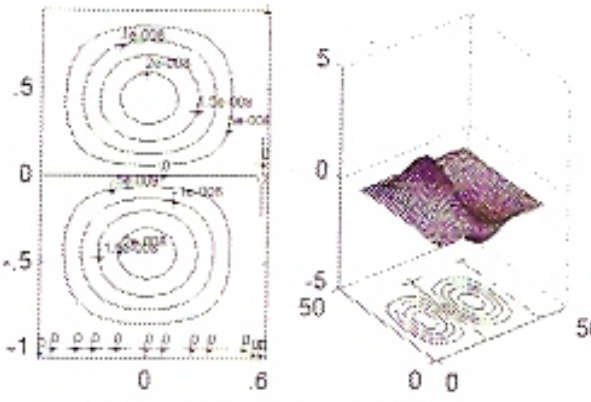

Fig.(60),paths of particales projected on the cross-section for β=0.024,k=1.77,L=0.01, τ=1.57

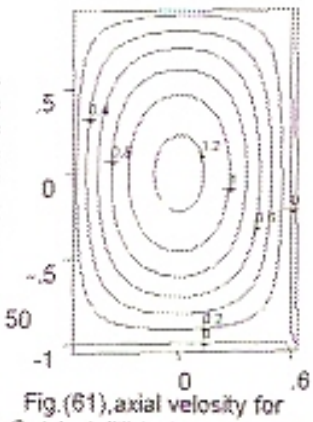

Fig.(61),axial velosity for β=1,k=1.77,L=0.01, τ=0.39

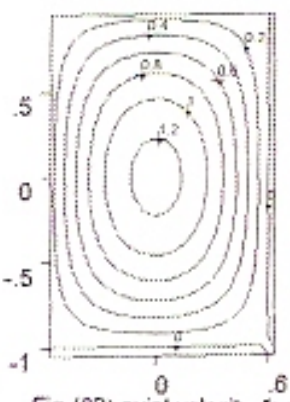

Fig.(62),axial velosity for β=2,k=1.77,L=0.01, τ=0.39

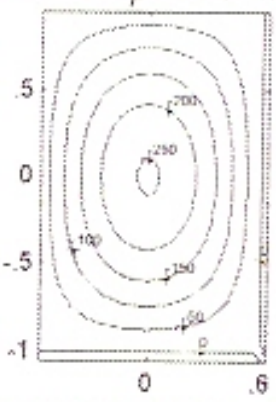

Fig.(63),axial velosity for β=1,k=5.1,L=0.01,τ=0.39

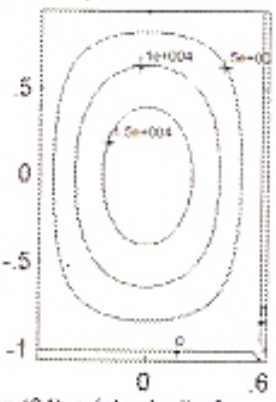

Fig.(64),axial velosity for β=1,k=9,L=0.01, τ=0.39

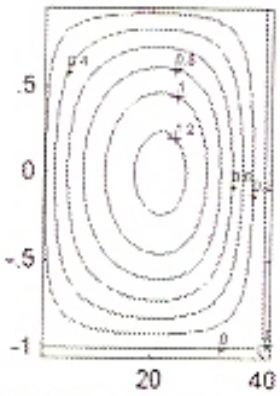

Fig.(65),axial velosity for β=1,k=1.77,L=3.36, τ=0.39

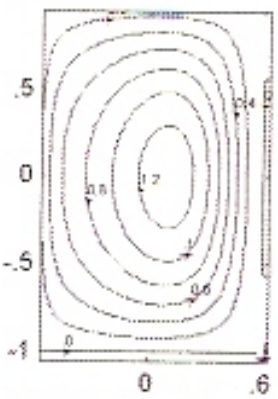

Fig.(66),axial velosity for β=1,k=1.77,L=8,τ=0.39

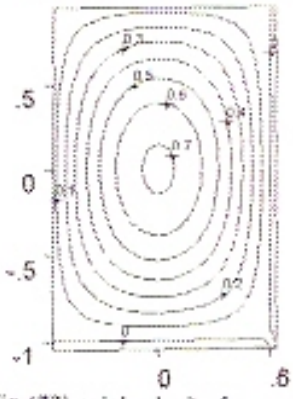

Fig.(67),axial velosity for β=1,k=1.77,L=0.01, τ=1.36

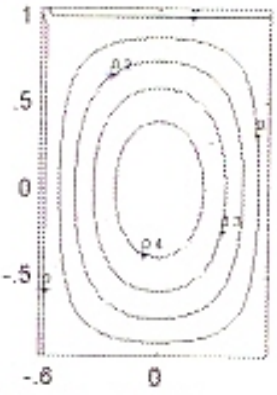

Fig.(68),axial velosity for β=1,k=1.77,L=0.01,τ=1.57

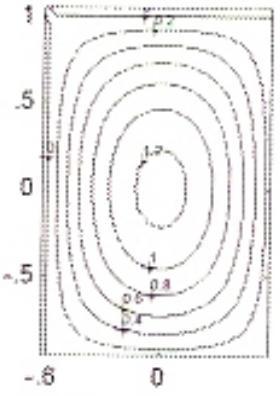

Fig.(69),axial velosity for β=0,k=1.77,L=0.01,τ=0.39

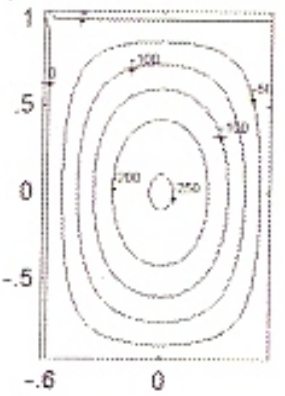

Fig.(70),axial velosity for β=0.024,k=5.1,L=0.01, τ=0.3

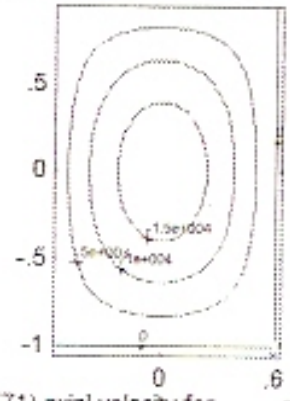

Fig.(71),axial velosity for β=0.024,k=9,L=0.01,τ=0.39

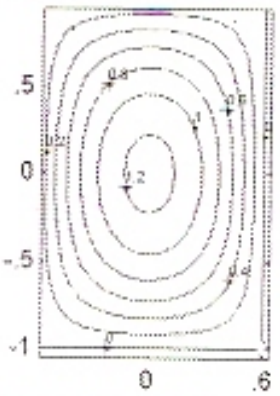

Fig.(72),axial velosity for β=0.024,k=1.77,L=3.36,τ=0.39

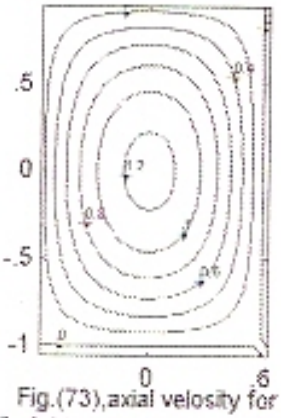

Fig.(73),axial velosity for β=0.024,k=1.77,L=8,τ=0.39

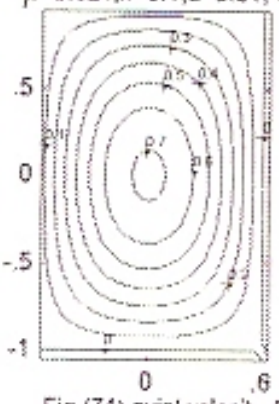

Fig.(74),axial velosity for β=0.024,k=1.77,L=0.01, τ=1.

References

1. Abdul-Hadi, A. M. (**2000**). *[Flow Analysis Through Curved Pipes]* Ph.D. Thesis Submitted to the University of Pune.
2. Al-Musawy A. Z. H. (**2004**). *[Flow of Non-Newtonian Fluid in Curved Pipe]*. M.Sc. Thesis Submitted to the University of Baghdad.
3. Atkinson, K., Han, W. (**2001**). *[Theoretical Numerical Analysis, a Functional Analysis Framework]*. Springer -Verlag New York, Inc.
4. Cheng K. C., Lin R. C. and Ou J. W. (**1976**). *[Fully Developed Laminar Flow in a Curved Rectangular Channel]* Trans ASME I: J. Fluids Engng Vol. 98 pp 41
5. Dean W. R. (**1927**). *[Note on the Motion of Fluid in a Curved Pipe]* Philos. Mag. Vol. 20. pp. 208.
6. Dean W. R. (**1928**). *[The Stream Line Motion of Fluid in a Curved Pipe]*. Philos. Mag. Vol. 30, pp. 673.
7. Dean W. R. and Hurst J. M. (**1959**). *[Note on the Motion of Fluid in Curved Pipe]*. Mathematika. Vol. 6, pp 77
8. Elsgolc , L.E (**1962**) *[Calculus of Variations]*. Pergamon press LTd.
9. Ghia K, N. and Sokhey J. S. (**1977**). *[Laminar Incompressible Viscous Flow in Curved Ducts of Regular Cross-Section]*. Trans ASME I: J. Fluids Engng Vol. 99 pp 640.
10. Jing-Wu wang and Andrews J. R. G. (**1995**). [*Numerical Simulation of Flow in Helical Duct*]. AIC'GE Journal Vol. 41 No. 5, PP. 1071.
11. Jones J. R.. (**1960**). *[Flow of a non-Newtonian liquid in a curved pipe]*. Quart. Journal. Mech. And Applied Math., Vol. XIII, pt4, pp.428.
12. Joseph B., Smith E. P. and Adler R. J. (**1975**). *[Numerical Treatment Of Laminar Flow in Helically Coiled Tubes of Square Cross-Section]* AICHE Journal, Vol. 21. No. 5. pp. 965.
13. Mori. Y., Uchida. Y. and Ukon T. (**1971**). *[Forced Convective Heat Transfer in a Curved Channel with a Square Cross-Section]* Intl. J. Heat Mass Transfer Vol. 4 pp. 1787.
14. Ravi Sankar S. Nandakumar K. and Masliya J. H. (**1988**). *[Oscillatory Flows In Coiled SquareDucts]*. Phys. Fluids Vol. 31 pp 1348.
15. Rektorys Karel. (**1980**). *[Variational Methods In Mathematics, Science And Engineering}*. D. Reiael publishing company.
16. Rivlin, R. S. (**1948**). *[The Hydrodynamics of Non-Newtonian Fluid].Proc.* Roy.Soc.A, Vol.193:pp. 260.
17. Thangam S. and Hur N. (**1990**). *[Laminar Secondary Flow In A Curved Rectangular Ducts]*. J. Fluid Mech. Vol. 217 pp.421.
18. Winter, K. H. (**1987**). *[A Bifurcation Study of Laminar Flow in a Curved Tube of RectangularCross-Section }* J. Fluid mech. Vol. 180. PP 343.
19. Ya khot, A., Arab, M., Ben-Dor, G. (**1999**). *[Numerical Investigation of a Laminar Pulsating Flow in a Retangular Duct.]*. J. Num. Math. Fluids, Vol. 29 PP 935-950.